

# What KM3-230213A events may tell us about the neutrino mass and dark matter

Basabendu Barman,<sup>1,\*</sup> Arindam Das,<sup>2,3,†</sup> and Prantik Sarmah<sup>4,‡</sup>

<sup>1</sup> *Department of Physics, School of Engineering and Sciences, SRM University-AP, Amaravati 522240, India*

<sup>2</sup> *Institute for the Advancement of Higher Education, Hokkaido University, Sapporo 060-0817, Japan*

<sup>3</sup> *Department of Physics, Hokkaido University, Sapporo 060-0810, Japan*

<sup>4</sup> *Institute of High Energy Physics, Chinese Academy of Sciences, Beijing, 100049, People's Republic of China*

Within the framework of general  $U(1)$  scenario, we demonstrate that the ultra high energy neutrinos recently detected by KM3NeT could originate from a decaying right handed neutrino dark matter (DM), with a mass of 440 PeV. Considering DM production via freeze-in, we delineate the parameter space that satisfies the observed relic abundance and also lies within the reach of multiple gravitational wave detectors. Our study provides a testable new physics scenario, enabled by multi-messenger astronomy.

**Introduction.**— The KM3NeT experiment recently reported the detection of event KM3-230213A [1], involving ultra high energy (UHE) neutrinos in the range  $110 \text{ PeV} \leq E_\nu \leq 790 \text{ PeV}$ , with a median energy of 220 PeV—the highest-energy neutrino observed on Earth to date. The experiment detected a UHE muon through its deep-sea neutrino telescope, with an energy of  $120_{-60}^{+110}$  PeV, arriving from an almost horizontal direction (RA :  $94.3^\circ$ , Dec :  $-7.8^\circ$ ). This muon is believed to have originated from a more energetic neutrino interacting near the detector. Such energetic neutrinos can be produced in cosmic-ray interactions, specifically via proton-proton and proton-photon collisions at standard astrophysical sources, where emission of photons associated with neutrinos is guaranteed. However, no such energetic source is known to exist within the Milky Way or nearby galaxies. The absence of compelling evidence pinpointing the origin of these UHE neutrinos, as observed by KM3NeT [2–4], raises the possibility that they have a cosmogenic origin. In particular, they could be produced via the Greisen-Zatsepin-Kuzmin (GZK) effect [5, 6], in association with UHE gamma rays, as predicted in various models [7–10]. However, the large uncertainty in the flux of event KM3-230213A—of order  $\mathcal{O}(3)$ —not only exceeds expectations from current UHE neutrino and gamma-ray flux models but also surpasses the sensitivities of IceCube and the Pierre Auger Observatory (PAO), where no similar event has been observed within a  $2.5\sigma$  to  $3\sigma$  significance range. This discrepancy challenges the cosmogenic neutrino hypothesis [11, 12], and calls for other possible explanations.

In [13], we investigated a decaying dark matter (DM) scenario to explain the origin of UHE neutrinos observed by IceCube. The detection of KM3NeT events prompts us to reconsider this framework<sup>1</sup>. Our scenario can be naturally embedded within a general anomaly-free  $U(1)$  extension of the Standard Model (SM), incorporating

three right-handed neutrinos (RHNs) [32] and a beyond-the-Standard-Model (BSM) scalar singlet. The BSM scalar acquires a nonzero vacuum expectation value (VEV), generating Majorana masses for the RHNs and breaking the  $U(1)_X$  symmetry, thereby inducing the seesaw mechanism, which gives rise to tiny neutrino masses and flavor mixing [33–39]. We consider a long-lived decaying DM candidate, that can be identified as the lightest RHN with a mass in the PeV range, depending on the neutrino mass hierarchy—either normal (NH) or inverted (IH). By fitting neutrino oscillation data [40], we estimate the DM lifetime for both NH and IH cases and use this to reproduce the expected neutrino and photon fluxes at KM3NeT [2–4]. This PeV-scale decaying DM, which explains the origin of UHE neutrino event with  $\langle E_\nu \rangle \simeq 220 \text{ PeV}$ , could be produced via the freeze-in mechanism [41]. The breaking of  $U(1)_X$  symmetry also leads to the formation of one-dimensional topological defects in the form of cosmic strings (CS) [42, 43], characterized by a string tension  $G\mu \sim \mathbb{B} Gv_\Phi^2$ , where  $v_\Phi$  is the VEV of the  $U(1)_X$  symmetry-breaking singlet scalar, and  $\mathbb{B} \sim 0.1$  [44–46]. Thus, this scenario provides a compelling framework in which the KM3NeT event not only provides a hint towards decaying DM, but sheds light on the neutrino mass hierarchy as well. Moreover, the gravitational waves (GWs) from cosmic strings predicted in this scenario could be probed by several proposed GW detectors. Finally, we constrain very heavy  $Z'$ , that acquires mass via spontaneous breaking of  $U(1)_X$ , from KM3-230213A events, DM abundance and GW from CS. Such heavy gauge bosons are beyond the scope of existing direct search experiments.

**The model framework**— Under the  $\text{SM} \otimes U(1)_X$  gauge symmetry, the SM quarks transform as  $q_L^i = \{3, 2, \frac{1}{6}, \frac{1}{6}x_H + \frac{1}{3}x_\Phi\}$ ,  $u_R^i = \{3, 1, \frac{2}{3}, \frac{2}{3}x_H + \frac{1}{3}x_\Phi\}$ ,  $d_R^i = \{3, 1, -\frac{1}{3}, -\frac{1}{3}x_H + \frac{1}{3}x_\Phi\}$ , respectively. The SM leptons transform as  $\ell_L^i = \{1, 2, -\frac{1}{2}, -\frac{1}{2}x_H - x_\Phi\}$ ,  $e_R^i = \{1, 1, -1, -x_H - x_\Phi\}$ , respectively, while the SM Higgs transforms as  $H = \{1, 2, \frac{1}{2}, \frac{x_H}{2}\}$ . Three SM-singlet RHNs species, required to cancel gauge and mixed gauge-gravity anomalies, transform as  $N_R^i = \{1, 1, 0, -x_\Phi\}$  with

<sup>1</sup> Other possible new physics explanation for KM3NeT events can be found in [11, 14–31].

$i = 1, 2, 3$  and one SM-singlet  $U(1)_X$  scalar transforms as  $\Phi = \{1, 1, 0, 2x_\Phi\}$ . The Yukawa interactions relevant for the neutrino mass can be written as

$$\mathcal{L} \supset -Y_{\nu_{\alpha\beta}} \bar{\ell}_L^\alpha \tilde{H} N_R^\beta - \frac{1}{2} Y_{N_\beta} \Phi \overline{(N_R^\beta)^c} N_R^\beta + \text{H.c.}, \quad (1)$$

where we consider a basis where  $Y_{N_\alpha}$  is a diagonal matrix, and  $\tilde{H} = i\tau^2 H^*$  with  $\tau^2$  being the second Pauli matrix. The scalar potential of this scenario is given by

$$V = \sum_{\mathcal{I}=H,\Phi} \left[ m_{\mathcal{I}}^2 (\mathcal{I}^\dagger \mathcal{I}) + \lambda_{\mathcal{I}} (\mathcal{I}^\dagger \mathcal{I})^2 \right] + \lambda_{\text{mix}} (H^\dagger H) (\Phi^\dagger \Phi). \quad (2)$$

After the breaking of  $U(1)_X$  and electroweak gauge symmetries, the scalar fields  $H$  and  $\Phi$  develop their VEVs as

$$\langle H \rangle = \frac{1}{\sqrt{2}} \begin{pmatrix} v+h \\ 0 \end{pmatrix}, \quad \text{and} \quad \langle \Phi \rangle = \frac{v_\Phi + \phi}{\sqrt{2}}, \quad (3)$$

where electroweak scale is  $v = 246$  GeV at the potential minimum. In the limit  $v_\Phi \gg v$ , the mass of the  $U(1)_X$  gauge boson can be written as  $M_{Z'} = 2g_X x_\Phi v_\Phi$ . Due to  $U(1)_X$  gauge symmetry the partial decay widths of  $Z'$  into a pair of SM fermions and RHNs will depend on  $x_H$  and  $x_\Phi$ . The corresponding partial decay widths are given in the Sec. I of the supplemental material. Taking  $x_\Phi = 1$  without the loss of generality we find that for  $x_H = -2$ ,  $\ell_\ell$  and  $q_\ell$  do not have interactions with  $Z'$ , for  $x_H = 0$  left and right handed SM fermions interact equally with  $Z'$  which provides the B–L scenario and finally for  $x_H = -1$ ,  $e_R$  does not interact with  $Z'$ . The breaking of  $U(1)_X$  and electroweak symmetries induce the Majorana mass term for the RHNs and the Dirac mass term for the light left-handed neutrinos from Eq. (1) as

$$m_{D_{\alpha\beta}} = \frac{Y_{\nu_{\alpha\beta}}}{\sqrt{2}} v, \quad M_{N_\beta} = \frac{Y_{N_\beta}}{\sqrt{2}} v_\Phi. \quad (4)$$

Hence light active neutrino masses can be derived using the standard see-saw formula

$$m_\nu \simeq -m_D M_N^{-1} m_D^T, \quad (5)$$

which successfully explains the tiny neutrino masses and their flavor mixing. Diagonalizing Eq. (5) we obtain

$$\mathcal{U}^T m_\nu \mathcal{U} = \text{diag}(m_1, m_2, m_3). \quad (6)$$

where  $\mathcal{U}$  is the PMNS matrix and it depends on neutrino oscillation data [40]. We consider the light neutrino mass eigenvalues follow  $m_1 = m_{\text{lightest}} < m_2 < m_3$  in NH and  $m_3 = m_{\text{lightest}} < m_1 < m_2$  in IH scenarios where  $m_{\text{lightest}}$  is the lightest light neutrino mass being a very small free parameter. From the seesaw formula we write

$$V_{\alpha\beta}^{\text{NH(IH)}} = \mathcal{U}^* \sqrt{D^{\text{NH(IH)}}} \sqrt{M_N^{-1}}, \quad (7)$$

when  $M_N$  is in diagonal basis for the normal (NH) and inverted (IH) hierarchies of the neutrino mass. All matrices and their dependence on neutrino oscillation data are written in Sec. II of supplemental materials. From the definition of neutrino mixing

$$V_{\alpha\beta}^{\text{NH(IH)}} = m_{D_{\alpha\beta}}^{\text{NH(IH)}} / M_{N_\beta} = \frac{Y_{\nu_{\alpha\beta}}^{\text{NH(IH)}} v}{\sqrt{2} M_{N_\beta}}. \quad (8)$$

Out of three RHN species, we identify the lightest RHN ( $N_\beta$ ) species ( $N_{1(3)}$  in NH(IH)) as a long-lived decaying DM candidate ensured by the corresponding Yukawa coupling ( $Y_{\nu_{\alpha\beta}}^{\text{NH(IH)}}$ ) which mixes  $N_\beta$  with the light neutrinos after electroweak symmetry breaking where  $N_\beta$  has dominant tree-level decays following  $N_\beta \rightarrow \ell_\alpha^\mp W^\pm$ ,  $\nu_\alpha Z$  and  $\nu_\alpha h$  where  $h$  is the SM-like Higgs. The partial decay widths of RHNs contain suppression factor of  $\mathcal{O}(1/M_{N_\beta}^2)$  [47] allowing us to neglect the effect of the masses of the SM bosons and hence we write the two-body partial decay widths of  $N_\beta$  as

$$\Gamma(N_\beta \rightarrow \ell_\alpha^- W^+) \simeq \frac{|Y_{\nu_{\alpha\beta}}^{\text{NH(IH)}}|^2 M_{N_\beta}}{32\pi},$$

$$\Gamma(N_\beta \rightarrow \nu_\alpha Z) = \Gamma(N_\beta \rightarrow \nu_\alpha h) \simeq \frac{|Y_{\nu_{\alpha\beta}}^{\text{NH(IH)}}|^2 M_{N_\beta}}{64\pi}. \quad (9)$$

The radiative decay mode  $N_\beta \rightarrow \gamma \nu_\alpha$  [48, 49] can be approximated as

$$\Gamma_{N_\beta \rightarrow \gamma \nu_\alpha} \simeq \frac{9 G_F^2 \alpha_{\text{EM}}}{2048 \pi^4} |Y_{\nu_{\alpha\beta}}^{\text{NH(IH)}}|^2 v^2 M_{N_\beta}^3, \quad (10)$$

where  $\alpha_{\text{EM}} = 1/137$  and  $G_F = 1.166 \times 10^{-5}$  GeV<sup>-2</sup> are the fine structure constant and Fermi constant, respectively.

In the context of KM3-230213A,  $N_{1(3)}$  could be a potential DM candidate for the NH (IH) case. The DM lifetime, including all possible two-body decays, reads

$$\tau_{\text{DM}}^{\text{NH(IH)}} \approx (3 \times 10^{29} \text{ s}) \left( \frac{440 \text{ PeV}}{M_{1(3)}} \right)^3 \left( \sum_\alpha \left| \frac{Y_{\nu_{\alpha 1(3)}}^{\text{NH(IH)}}}{10^{34}} \right|^2 \right)^{-1}. \quad (11)$$

Fitting the neutrino oscillation data in Eqs. (7) and (8) we find  $Y_{21}^{\text{NH}} \simeq 6.3 \times 10^{-35}$  and  $Y_{23}^{\text{IH}} \simeq 2.4 \times 10^{-34}$  are the corresponding Yukawa couplings between the DM and  $\nu_\mu$  by defining the lightest light neutrino mass as  $m_{\text{lightest}} = r \sqrt{\Delta m_{12}^2} = 1.62(8.71) \times 10^{-72}$  GeV for NH (IH). We consider  $r$  as a free parameter of benchmark values  $1.86 \times 10^{-61}$  and  $10^{-60}$  for NH and IH cases, respectively. Using these couplings we obtain DM lifetime using Eq. (11) as  $\tau_{\text{DM}}^{\text{NH(IH)}} = 7 \times 10^{29} (5 \times 10^{28})$  s. In Fig. 1 we show the DM lifetime as a function of the DM mass. Since  $\tau_{\text{DM}} \propto M_{1(3)}^{-3}$ , hence the lifetime shortens with the increase in DM mass. The benchmark points for NH and IH are shown for a DM mass of 440

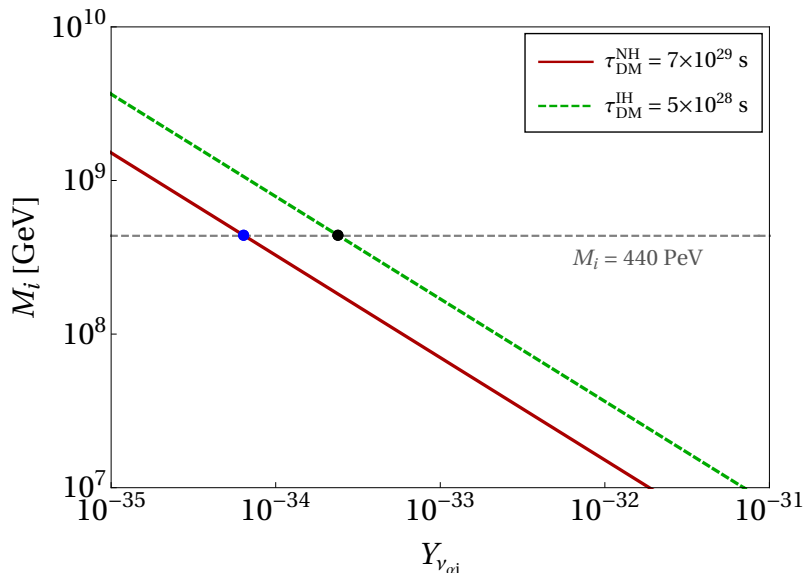


Figure 1. Contours corresponding to DM lifetime, considering all decay channels where points correspond to benchmark Yukawa values for NH (IH) in blue(black) cases respectively for decay into muonic final states.

PeV.

### Dark matter induced explanation of the excess

The decay of heavy RHN DM can yield high energy secondaries, i.e, gamma-rays and neutrinos in the final state. To compute the flux of these secondaries from decaying DM in Milky Way, we require the density profile of the Milky Way DM halo. While there are several different models of the DM profile in the literature [50–54], we choose the extensively explored Navarro-Frenk-White (NFW) [50, 51] density profile for this work. The DM density in Milky Way as a function of the Galactocentric radius ( $R_{GC}$ ) is given by the NFW profile as,

$$\rho_{\text{dm}} = \rho_{\text{NFW}}(R_{GC}) = \frac{\rho_C}{(R_{GC}/R_C)(1 + R_{GC}/R_C)^2}, \quad (12)$$

where,  $R_C = 11$  kpc and  $\rho_C$  are the characteristic scale and density, respectively.  $\rho_C$  is obtained by normalizing the DM profile to the DM density at solar neighbourhood,  $\rho_{\odot} = 0.43 \text{ GeV cm}^{-3}$ . The flux of secondary gamma-rays and neutrinos can be obtained by estimating the amount of DM in the angular region,  $\Delta\Omega$  of observation and given by,

$$\mathcal{D} = \frac{1}{\Delta\Omega} \int_{\Delta\Omega} d\Omega \int_0^{s_{\text{max}}} ds \rho_{\text{dm}}(s, b, l). \quad (13)$$

Here,  $s$  is the line of sight distance which is connected to the Galactic longitude ( $l$ ) and latitude ( $b$ ) by the relation  $r = \sqrt{s^2 + R_{\odot}^2 + 2sR_{\odot} \cos b \cos l}$ , where  $R_{\odot} = 8.3$  kpc is the distance to the Milky Way center from the Sun. The flux of the secondaries given by,

$$\frac{d^2\phi_{i,G}(E_i)}{dE_i d\Omega} = \frac{\mathcal{D}}{4\pi M_{\text{dm}} \tau_{\text{dm}}} \frac{dN_i(E_i)}{dE_i}, \quad (14)$$

where,  $i$  represents gamma-rays or neutrinos of any specific flavor. In addition to the Galactic DM, extra-galactic DM can also contribute to the high-energy gamma-ray and neutrino fluxes, which can be obtained by the following formula,

$$\frac{d\phi_{i,EG}(E_i)}{dE_i} = \frac{c \rho_{\text{dm}}}{4\pi M_{\text{dm}} \tau_{\text{dm}}} \int dz \left| \frac{dt}{dz} \right| \frac{dN(E'_i)}{dE'_i} e^{-\tau_{\text{OD}}(E'_i, z)}, \quad (15)$$

where  $E'_i = E_i(1+z)$  corresponds to the energy of the  $i^{\text{th}}$  particle at redshift  $z$ . The DM density is given by  $\rho_{\text{DM}} = \Omega_{\text{DM}} \rho_c$ , where  $\rho_c = 4.7 \times 10^{-6} \text{ GeV cm}^{-3}$  is the critical DM density in a flat Friedmann–Lemaître–Robertson–Walker (FLRW) Universe and  $\Omega_{\text{DM}} = 0.27$ . The cosmological line element,  $\left| \frac{dt}{dz} \right|$  can be expressed as

$$\left| \frac{dt}{dz} \right| = \frac{1}{\mathcal{H}_0(1+z)\sqrt{(1+z)^3\Omega_m + \Omega_\Lambda}}, \quad (16)$$

where  $\Omega_m = 0.315$ ,  $\Omega_\Lambda = 0.685$  and  $\mathcal{H}_0 = 67.3 \text{ km s}^{-1} \text{ Mpc}^{-1}$  is the current expansion rate of the Universe. The factor  $e^{-\tau(E', z)}$  takes into account of the attenuation of the gamma-ray flux due to pair production losses in the extra-galactic background light (EBL) and CMB during propagation, where  $\tau_{\text{OD}}(E', z)$  is the total optical depth of EBL and CMB. The optical depth (OD) of EBL is taken from [55]. The term  $dN_i/dE_i$  in Eq. (14) and Eq. (15) represents the differential spectra of secondary gamma-rays and neutrinos as a function of energy,  $E_i$  and obtained from the publicly available code `HDMSpectra` [56].

The total flux,  $\phi_i$  is obtained by the summing over both the Galactic and extra-galactic components. The

total flux depends on the two free parameters, namely, the DM mass  $M_{\text{dm}}$  and the DM lifetime  $\tau_{\text{dm}}$ . The mass of the decaying DM can be fixed by kinematics of two body decay to 440 PeV. For constraining  $\tau_{\text{dm}}$ , we consider gamma-ray observations by different telescopes across a broad energy band, ( $10^1 - 10^6$ ) TeV. In the lower energies,  $E_\gamma < 10^3$  TeV, we adopt the diffuse flux measurements from the inner Galactic plane ( $15^\circ < l < 125^\circ$  and  $-5^\circ < b < 5^\circ$ ) by the Kilometer Square Array at the Large High Altitude Air Shower Observatory (LHAASO-KM2A) [57]. For higher energies, we constrain the gamma-ray flux from DM decay using the upper limits on UHE photon flux from Moscow State University Extensive Air Shower (EAS-MSU) array [58] and Pierre Auger Observatory (PAO HECO +SD750) [59].

The gamma-ray flux from the decay of  $N_1$  (assuming NH) is represented by the solid purple curve in Fig. 2. This flux is calculated for the inner Galactic plane. For comparison, we also include gamma-ray data from LHAASO-KM2A (orange data points), EAS-MSU (maroon downward arrows), and PAO HECO + SD750 (brown downward arrows). To remain consistent with these observations, the dark matter (DM) lifetime is set to  $7 \times 10^{29}$  s. The muon neutrino flux from  $N_1$  decay, computed for the angular region constrained by the uncertainty in the arrival direction of KM3-230213A, is shown as the solid green curve. We account for neutrino oscillations during propagation, leading to a final neutrino flavor ratio at Earth of 3 : 2 : 1 for NH and 1 : 2 : 3 for IH. Consequently, the muon neutrino flux after oscillations remains similar in both cases. While the predicted neutrino flux is over an order of magnitude lower than the central flux value of the KM3-230213A event, it still lies within its  $3\sigma$  uncertainty. Thus, a DM origin for the KM3-230213A event cannot be completely ruled out. For consistency with existing observations, we also display IceCube’s High Energy Starting Events (HESE) [60] as cyan data points. In the IH scenario,  $N_3$  serves as the potential DM candidate. The gamma-ray and neutrino fluxes from  $N_3$  decay are shown as the dashed purple and dashed green curves, respectively. Here, the DM lifetime is taken as  $5 \times 10^{28}$  s, following the benchmark value in Fig. 1. While the resulting neutrino flux is close to the central value of KM3-230213A, the corresponding gamma-ray flux is in tension with the observed gamma-ray data. It is important to note that the choice of DM lifetime is not unique, by adjusting the Yukawa parametrization, one can fine-tune the gamma-ray flux to match observations.

We further estimate the expected number of muon neutrino events in KM3NeT for our predicted neutrino flux from DM decay. The number of events  $N_{\text{event}}$  in the energy interval  $\Delta E_{\nu_\mu}$  is given by,

$$N_{\text{event}} = \mathcal{T}_{\text{obs}} \int_{E_{\nu_\mu}}^{E_{\nu_\mu} + \Delta E_{\nu_\mu}} dE_{\nu_\mu} \frac{d\phi_{\nu_\mu}}{dE_{\nu_\mu}} \mathcal{A}_{\text{eff}}(E_{\nu_\mu}), \quad (17)$$

where  $\mathcal{T}_{\text{obs}}$  is the observation time and  $\mathcal{A}_{\text{eff}}(E_{\nu_\mu})$  is the effective area of KM3NeT detector for muon neutrinos [61]. For the computation of the events, we consider the diffuse flux integrated over the entire Galactic DM halo. In the left panel of Fig. 3, we show the expected number of events (black line) as a function energy for a observation time of 10 years. The gray band shows the  $1\sigma$  spread in the events considering Poisson statistics, i.e.,  $\sigma = \sqrt{N_{\text{event}}}$ . In addition, we show the variation of the total events integrated in the energy range 5 TeV to  $5 \times 10^5$  TeV with respect to  $\tau_{\text{dm}}$  in the right panel. The gray band corresponds to the  $1\sigma$  uncertainty, and the red horizontal line corresponds to 1 event. As it is evident, KM3NeT will be able to probe  $\tau_{\text{dm}}$  up to around  $10^{31}$  s after 10 years of observation.

**Dark matter genesis**– Dark matter (DM) in the form of PeV-scale  $N_{1(3)}$  for NH (IH) can be produced via freeze-in through the following mechanisms: (i) the on-shell decay of  $Z'$ , provided that  $M_{Z'} > 2 M_{1(3)}$ ; (ii) the on-shell decay of  $\phi$ , if  $m_\phi > 2 M_{1(3)}$ ; and (iii)  $2 \rightarrow 2$  scattering of thermal bath particles mediated by  $Z'$ . The coupling strength  $g_X$  must be sufficiently small to ensure non-thermal DM production via freeze-in. Consequently,  $Z'$  never attains thermal equilibrium, and its comoving number density must be determined by solving a set of coupled Boltzmann equations (BEQs), given in Sec. IV of the supplemental material. We assume the mixing between  $\phi$  and  $h$  is negligibly small, and therefore,  $\phi$ -mediated scatterings and its decay into SM particles will be highly suppressed resulting not to consider their effects<sup>2</sup>. As a result,  $\phi$ —which remains part of the thermal bath—predominantly decays into RHNs and  $Z'$  in pairs. To fit the observed DM relic density, it is required that  $y_0 M_{1(3)} = \Omega h^2 \frac{1}{s_0} \frac{\rho_c}{h^2} \simeq 4.3 \times 10^{-10}$  GeV, where  $y_0 \equiv y_{N_{1(3)}}(z \rightarrow \infty)$  is the present DM yield. We use the critical energy density  $\rho_c \simeq 1.05 \times 10^{-5} h^2$  GeV/cm<sup>3</sup>, present entropy density  $s_0 \simeq 2.69 \times 10^3$  cm<sup>-3</sup> [66] and DM relic abundance  $\Omega h^2 \simeq 0.12$ , with  $h \simeq H_0/100$  (km/s/Mpc) being the reduced Hubble rate, where  $H_0 \simeq 67.4 \pm 0.5$  km/s/Mpc is the current Hubble rate [67].

The DM yield, as a function of  $z = M_{1(3)}/T$  is shown in Fig. 4. In the present scenario,  $Z'$  is always produced from the on-shell 2-body decay  $\phi \rightarrow Z' Z'$ , therefore, in all cases we consider  $m_\phi > 2 M_{Z'}$ . For  $M_{1(3)} < M_{Z'}/2$ , as well as  $M_{1(3)} < m_\phi/2$ , DM is dominantly produced from decays, hence an extremely tiny  $g_X$  is required to satisfy the DM abundance. This situation is considered in the top left panel. The DM production shows a non-trivial dynamics here. This is because both  $Z'$

<sup>2</sup> For detailed studies on the effects of scalar interactions on DM freeze-in production, see [63–65].

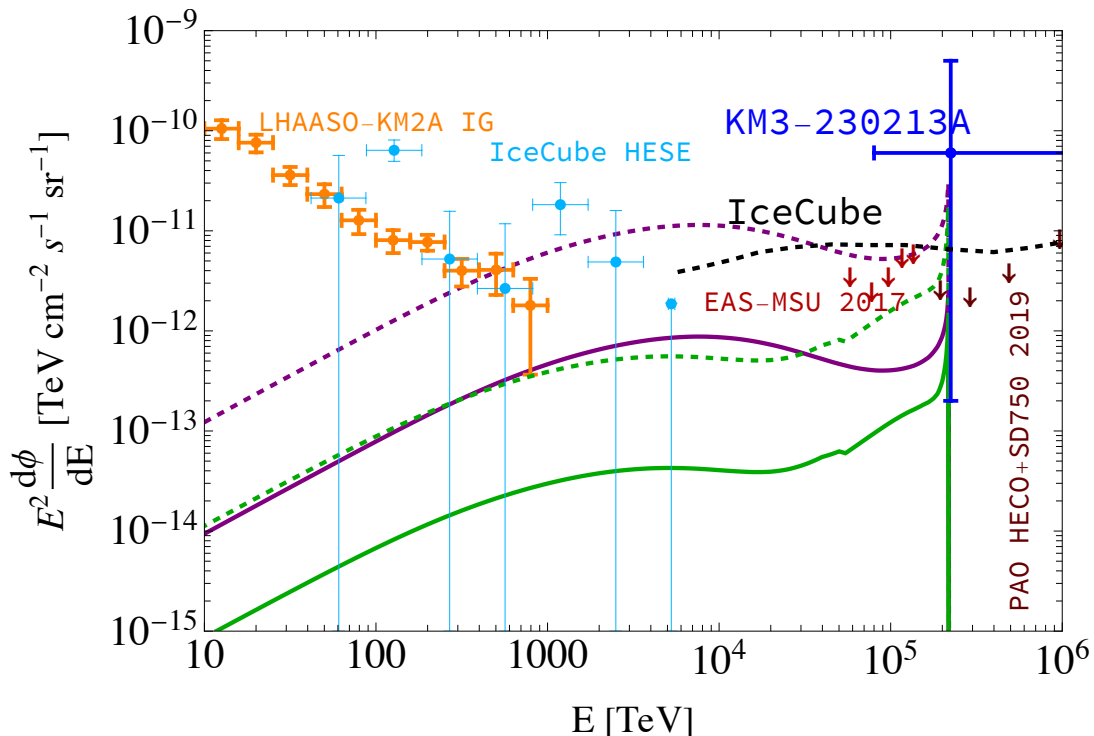


Figure 2. Gamma-ray (dashed curve) and muon neutrino (solid curve) flux for lifetime  $7 \times 10^{29}$  s (in purple) and  $5 \times 10^{28}$  s (in green), for NH and IH scenario respectively, compared with different experimental data. The mass of the DM is taken to be 440 PeV. The blue data point shows flux of the KM3NeT [1] event with  $3\sigma$  error bars. The light blue data points represent the IceCube HESE [60] data, whereas the black dotted curve shows the 90% CL sensitivity of IceCube [62] for cosmogenic neutrinos. The orange data point shows the measurement of diffuse gamma-rays from the inner Galactic (IG) plane by LHAASO [57]. The upper limits on UHE gamma-ray flux by Moscow State University Extensive Air Shower (EAS-MSU [58]) array and Pierre Auger Observatory (PAO HECO +SD750) [59] are shown by the maroon and brown downward arrows, respectively.

and DM yield builds up from  $\phi$ -decay. Since  $\phi$  decays (green dot-dashed curve) earlier compared to  $Z'$  (red dashed curve), hence the final DM abundance is set by  $Z'$ -decay. As a result, we notice a tiny bump at  $z \sim 3 \times 10^7$ , where  $Z'$  decay is completed, saturating the DM relic. In the top right panel, DM production dominantly takes place via  $\phi$ -decay since  $M_{1(3)} < m_\phi/2$  but  $M_{1(3)} > M_{Z'}$ . Once again, we see,  $g_X$  needs to be very feeble to produce the observed DM abundance. It is important to mention that  $g_X = 10^{-15}$  requires a Planckian  $v_\phi$  in order to satisfy  $M_{Z'} \geq 1$  TeV, and thus forbidden. For DM production entirely via  $Z'$ -mediated scattering, one requires  $M_{1(3)} > M_{Z'}, m_\phi$ . Here the DM freezes in at  $z \simeq 1$ , as shown in the bottom panel. This is the typical IR-feature of freeze-in, where the freeze-in happens at  $T = \max[M_{Z'}, M_{1(3)}]$ . Note that, in this case it is possible to have a much larger  $g_X$ , since scattering channels have a  $g_X^4$  dependence, compared to  $g_X^2$  dependence for decays.

**GW Spectrum from cosmic strings**– The primary mechanism of energy dissipation from cosmic strings (CS) is gravitational wave (GW) emission from oscillating loops, as demonstrated by numerical simulations based

on the Nambu-Goto action [68, 69]. The corresponding energy loss rate is given by [70]

$$P_{\text{GW}} = \frac{G}{5} (\ddot{Q})^2, \quad (18)$$

where  $Q$  represents the quadrupole moment of the oscillating loop, and its third time derivative scales as  $\ddot{Q} \propto \mu$ . Consequently, the energy loss rate follows as

$$\frac{dE}{dt} = -\Gamma G \mu^2, \quad (19)$$

where  $\Gamma \approx 50$  [71]. Due to the emission of GWs, the loop undergoes a gradual reduction in length from its initial value  $l_i = \alpha t_i$  at the formation time  $t_i$ , evolving as

$$l(t) = \alpha t_i - \Gamma G \mu (t - t_i), \quad (20)$$

where  $\alpha$  denotes the loop size parameter, which simulations suggest is approximately  $\alpha \approx 0.1$  [72, 73]. The total energy radiated by a loop is distributed among a series of normal mode oscillations, characterized by discrete frequencies

$$f_k = \frac{2k}{l(t)}, \quad (21)$$



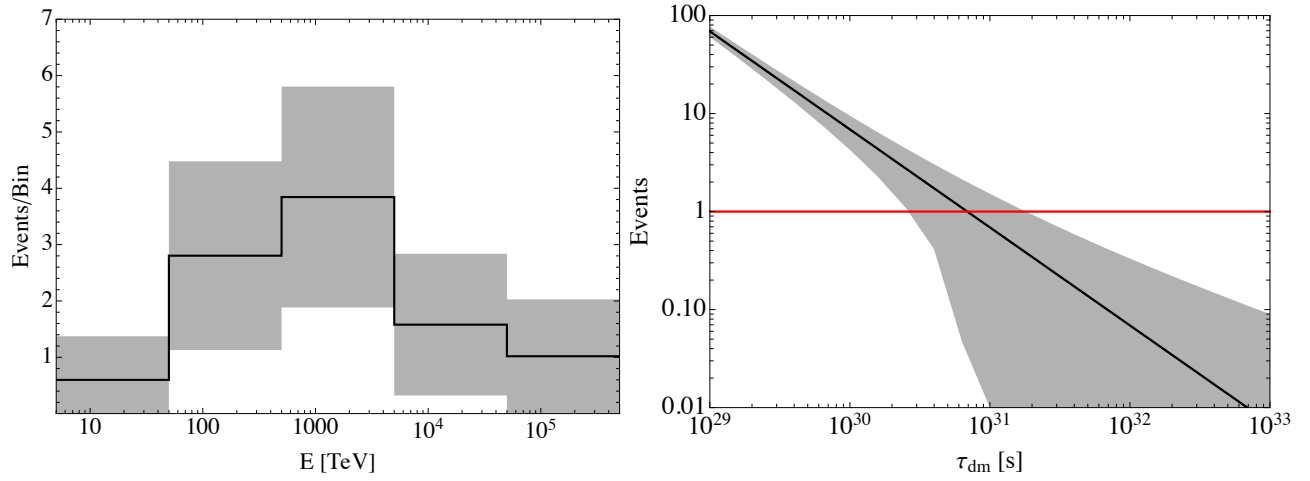


Figure 3. Left: Expected number of muon neutrino events in KM3NeT for a observation time of 10 years. Right: The gray band shows the  $1\sigma$  uncertainty in the events in Poisson statistics. The red straight line parallel to the horizontal axis marks 1 event counted by KM3NeT.

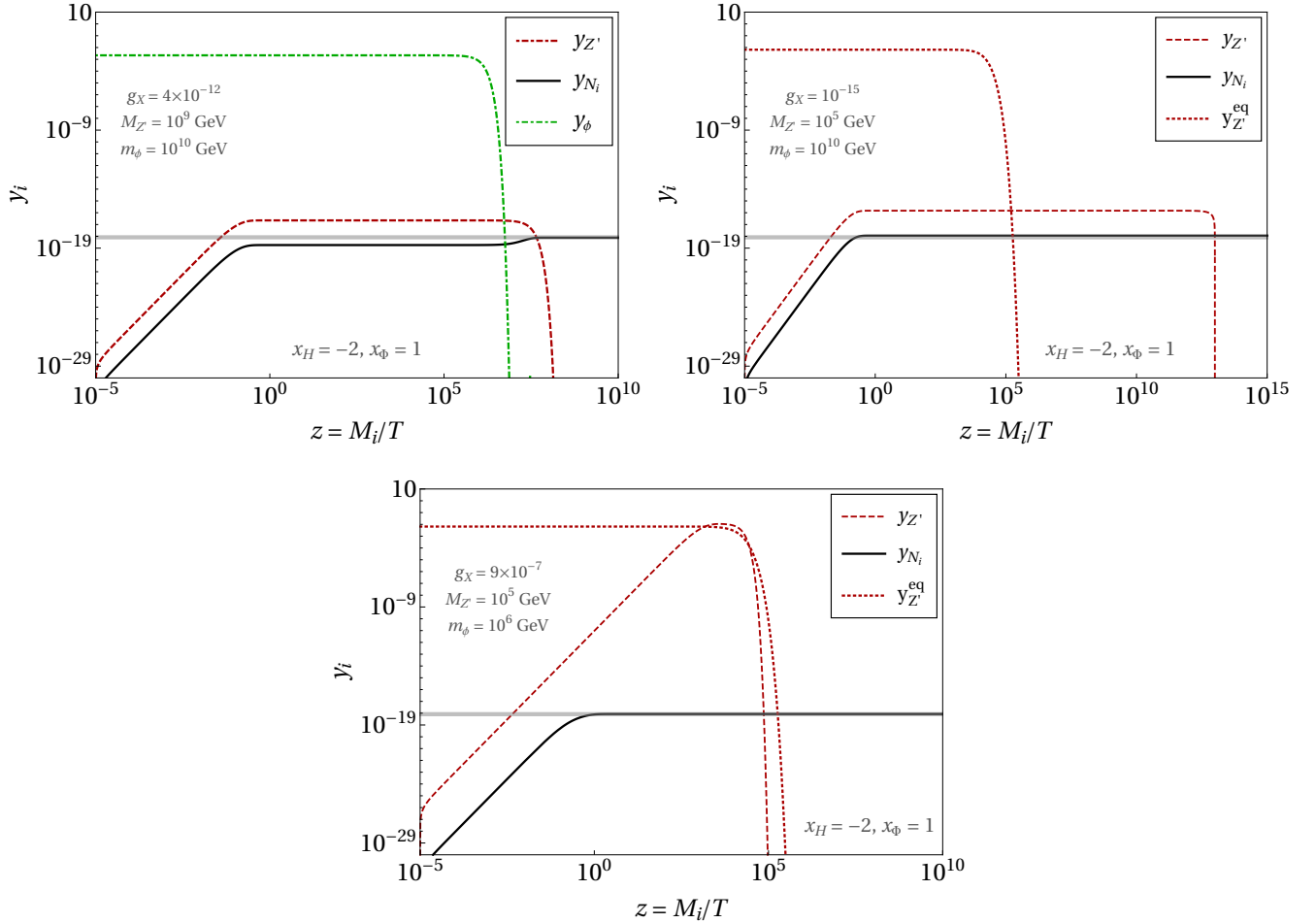


Figure 4. Evolution of DM yield (black solid curve), as a function of  $z = M_i/T$  with  $M_{1(3)} = 440$  PeV for NH (IH). Here we have chosen  $x_H = -2$ ,  $x_\phi = 1$  for illustration. In the top left panel DM is dominantly produced from the decay of both  $Z'$  and  $\phi$ , whereas the top right panel corresponds to DM production dominantly via  $\phi$ -decay. In the bottom panel DM is produced purely from  $Z'$ -mediated scattering. All relevant masses and couplings are mentioned in the plots.

where  $k$  represents the mode number ( $k = 1, 2, 3, \dots, \infty$ ).

The GW spectral density is expressed as

$$\Omega_{\text{GW}}(t_0, f) = \frac{f}{\rho_c} \frac{d\rho_{\text{GW}}(t_0, f)}{df} = \sum_k \Omega_{\text{GW}}^{(k)}(t_0, f), \quad (22)$$

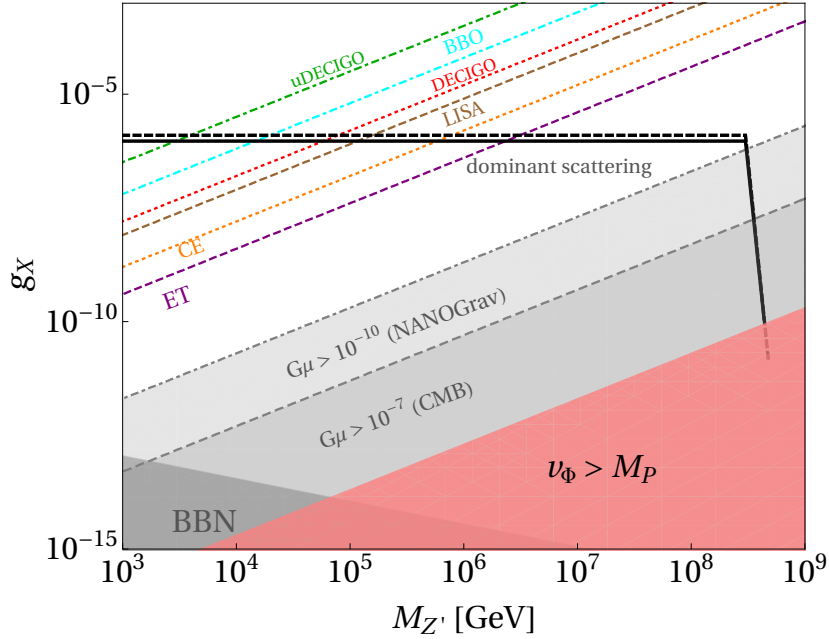


Figure 5. Contours of right relic abundance for a 440 PeV DM, shown by the solid black and dashed black curves, for  $x_H = \{-2, 0\}$ . Along the horizontal lines  $Z'$ -mediated scattering dominates. The diagonal dashed lines correspond to the sensitivity reach of several futuristic GW detectors. The shaded regions are disallowed from BBN bound on  $Z'$ -lifetime, requiring  $\tau_{Z'} \gtrsim 1$  sec, Planckian VEV values, CMB and NANOGrav bounds on CS tension (see text for details). DM production dominantly from  $\phi$ -decay requires  $v_\phi > M_P$ , hence *forbidden in this scenario*.

where  $f$  and  $t_0$  denote the present-day frequency and cosmic time, respectively. Since GW energy density redshifts as  $a^{-4}$ , we obtain [72]

$$\frac{d\rho_{\text{GW}}^{(k)}}{df} = \int_{t_F}^{t_0} \left[ \frac{a(t_E)}{a(t_0)} \right]^4 P_{\text{GW}}(t_E, f_k) \frac{dF}{df} dt_E, \quad (23)$$

where  $f_k$  denotes the frequency at emission ( $f_E$ ) at cosmic time  $t_E$ , with  $t_F$  representing the loop formation epoch. The factor  $\frac{dF}{df} = f \left[ \frac{a(t_0)}{a(t_E)} \right]$  accounts for the redshift of the frequency. The power radiated by the loops is given by

$$P_{\text{GW}}(t_E, f_k) = \frac{2k G \mu^2 \Gamma_k}{f \left[ \frac{a(t_0)}{a(t_E)} \right]^2} n \left( t_E, \frac{2k}{f} \left[ \frac{a(t_E)}{a(t_0)} \right] \right), \quad (24)$$

where  $\Gamma_k$  is defined as

$$\Gamma_k = \frac{\Gamma k^{-4/3}}{\sum_{m=1}^{\infty} m^{-4/3}}, \quad (25)$$

such that  $\sum_k \Gamma_k = \Gamma$ . The function  $n$ , number density of loops, depends on the background cosmology characterized by a scale factor  $a \propto t^\beta$ . Using the Velocity-Dependent One-Scale (VOS) model [74–76] and numerical simulations [72], the loop number density is given by

$$n(t_E, l_k(t_E)) = \frac{A_\beta}{\alpha} \frac{(\alpha + \Gamma G \mu)^{3(1-\beta)}}{[l_k(t_E) + \Gamma G \mu t_E]^{4-3\beta} t_E^{3\beta}}, \quad (26)$$

where  $A_\beta$  is a constant that depends on the cosmological background. The resulting GW spectrum is influenced by the small-scale structure of loops, which may feature cusps or kinks [77, 78]. Here we assume that cusp-like structures primarily govern the emitted GW spectrum.

Utilizing Eqs. (22)–(26), the present-day GW energy density for a given mode  $k$  is obtained as

$$\Omega_{\text{GW}}^{(k)}(t_0, f) = \frac{2k G \mu^2 \Gamma_k}{f \rho_c} \int_{t_{\text{osc}}}^{t_0} dt \left[ \frac{a(t)}{a(t_0)} \right]^5 n(t, l_k), \quad (27)$$

where the integration extends from  $t_{\text{osc}}$ , the epoch at which loops commence oscillations after being damped by thermal friction [79]. This damping phase is subdominant in its effect on the resulting GW spectrum.

For loops that form and radiate during the radiation-dominated era, the GW spectrum exhibits a characteristic flat plateau, with an amplitude given by

$$\Omega_{\text{GW}}^{(k=1), \text{plateau}}(f) = \frac{128\pi G \mu}{9\zeta(4/3)} \frac{A_r}{\epsilon_r} \Omega_r \left[ (1 + \epsilon_r)^{3/2} - 1 \right], \quad (28)$$

where  $\epsilon_r = \alpha / \Gamma G \mu$ , and  $A_r = 0.54$  [76] for the radiation-dominated universe.

**Results and discussions**– In Fig. 5 we show the relic density allowed parameter space for a 440 PeV DM. The thick and dashed contours correspond to  $x_H = \{-2, 0\}$ , respectively. We show the reach of proposed GW detectors: Big Bang Observer (BBO) [80, 81], ultimate DE-

CIGO (uDECIGO) [82, 83], LISA [84], the cosmic explorer (CE) [85] and the Einstein Telescope (ET) [86–89] in probing the parameter space, depending on  $v_\Phi$ . The light gray shaded region in the bottom left corner corresponds to  $\tau_{Z'} = 1/\Gamma_{Z'} > 1$  sec, that can potentially perturb the predictions of big bang nucleosynthesis (BBN). The darker red shaded region in the bottom right corner demands (super-)Planckian  $v_\Phi$ . Observations of the Cosmic Microwave Background (CMB) impose an upper limit on the string tension, requiring  $G\mu \lesssim 10^{-7}$  [90]. Under this constraint, the condition  $\alpha \gg \Gamma G\mu$  holds, leading to  $\Omega_{\text{GW}}^{(k=1)}(f) \propto v_\Phi$ . Recent results from NANOGrav [91] impose an even more stringent upper bound, limiting  $G\mu \lesssim 10^{-10}$ .

Now, along the horizontal branch of the black curves, the correct DM abundance is produced entirely via  $Z'$ -mediated scattering. Along these lines, we consider  $m_\phi = 10^6$  GeV, ensuring  $m_\phi < 2M_{1(3)}$  while maintaining  $m_\phi > 2M_{Z'}$ . For  $M_{Z'} \simeq 5 \times 10^7$  GeV, we set  $m_\phi = 10^9$  GeV, ensuring that the decay channel  $\phi \rightarrow Z'Z'$  is kinematically allowed. Since now  $m_\phi > 2M_{1(3)}$ , all decay channels become accessible, thereby requiring an extremely small  $g_X$ , as observed in the top panel of Fig. 4. We find  $g_X \simeq \{9 \times 10^{-7}, 10^{-6}\}$ , corresponding to  $x_H = \{-2, 0\}$  for DM production via  $Z'$ -scattering being independent of neutrino hierarchy as the DM mass is same in both the cases. For dominant DM production from  $\phi$  decay,  $g_X \lesssim \mathcal{O}(10^{-15})$  is required for  $M_{Z'} \gtrsim 1$  TeV, which implies  $v_\Phi \sim M_P$ , thereby excluding this possibility. Since a similar bound is obtained for  $x_H = 0$ , we do not explicitly show this case. For DM production purely via  $Z'$ -mediated scattering, we note, in the present framework, KM3NeT provides a slightly stronger bound than IceCube, where latter demands a decaying DM of mass 4 PeV [92, 93]. This can be understood from the fact that since in this case the final DM yield is largely independent of the mediator mass, hence one can write,  $(g_X^{\text{KM3}}/g_X^{\text{ice}}) \sim (4/440)^{1/4} \simeq 0.3$ , for  $x_H = 0$ .

**Conclusions**– The detection of a flux of UHE neutrinos by the deep-sea neutrino telescope KM3NeT opens a new avenue for investigating high-energy astrophysical sources, both Galactic and extragalactic. Additionally, it offers a powerful tool for constraining physics beyond the SM. This letter presents a minimal particle physics framework in which the origin of these high-energy neutrinos is linked to the decay of a PeV-scale fermionic DM candidate depending on neutrino mass hierarchy. This, in turn, imposes constraints on the mass and coupling of the new neutral gauge boson within the theory. Furthermore, we demonstrate that the viable DM parameter space, satisfying the KM3NeT events, lies within the sensitivity range of multiple gravitational wave detectors, highlighting a valuable complementarity

in the quest for searching new physics.

**Acknowledgments**– BB would like to acknowledge fruitful discussions with Suruj Jyoti Das. PS thanks Nayan Das for sharing some data used in the paper.

---

\* basabendu.b@srmmap.edu.in

† arindamdas@oia.hokudai.ac.jp

‡ prantiksarmah@ihep.ac.cn

- [1] **KM3NeT** Collaboration, S. Aiello *et al.*, “Observation of an ultra-high-energy cosmic neutrino with KM3NeT,” *Nature* **638** no. 8050, (2025) 376–382.
- [2] **KM3NeT, MessMapp Group, Fermi-LAT, Owens Valley Radio Observatory 40-m Telescope Group, SVOM** Collaboration, O. Adriani *et al.*, “Characterising Candidate Blazar Counterparts of the Ultra-High-Energy Event KM3-230213A,” [arXiv:2502.08484 \[astro-ph.HE\]](#).
- [3] **KM3NeT** Collaboration, O. Adriani *et al.*, “On the Potential Galactic Origin of the Ultra-High-Energy Event KM3-230213A,” [arXiv:2502.08387 \[astro-ph.HE\]](#).
- [4] **KM3NeT** Collaboration, O. Adriani *et al.*, “On the potential cosmogenic origin of the ultra-high-energy event KM3-230213A,” [arXiv:2502.08508 \[astro-ph.HE\]](#).
- [5] K. Greisen, “End to the cosmic ray spectrum?,” *Phys. Rev. Lett.* **16** (1966) 748–750.
- [6] G. T. Zatsepin and V. A. Kuzmin, “Upper limit of the spectrum of cosmic rays,” *JETP Lett.* **4** (1966) 78–80.
- [7] G. Gelmini, O. E. Kalashev, and D. V. Semikoz, “GZK photons as ultra high energy cosmic rays,” *J. Exp. Theor. Phys.* **106** (2008) 1061–1082, [arXiv:astro-ph/0506128](#).
- [8] R. Aloisio, D. Boncioli, A. di Matteo, A. F. Grillo, S. Petrerá, and F. Salamida, “Cosmogenic neutrinos and ultra-high energy cosmic ray models,” *JCAP* **10** (2015) 006, [arXiv:1505.04020 \[astro-ph.HE\]](#).
- [9] G. B. Gelmini, O. Kalashev, and D. Semikoz, “Upper Limit on the Diffuse Radio Background from GZK Photon Observation,” *Universe* **8** no. 8, (2022) 402, [arXiv:2206.00408 \[astro-ph.HE\]](#).
- [10] S. Chakraborty, P. Mehta, and P. Sarmah, “A relook at the GZK neutrino-photon connection: impact of extra-galactic radio background & UHECR properties,” *JCAP* **01** (2024) 058, [arXiv:2307.15667 \[astro-ph.HE\]](#).
- [11] S. W. Li, P. Machado, D. Naredo-Tuero, and T. Schwemberger, “Clash of the Titans: ultra-high energy KM3NeT event versus IceCube data,” [arXiv:2502.04508 \[astro-ph.HE\]](#).
- [12] **KM3NeT** Collaboration, O. Adriani *et al.*, “The ultra-high-energy event KM3-230213A within the global neutrino landscape,” [arXiv:2502.08173 \[astro-ph.HE\]](#).
- [13] B. Barman, A. Das, S. Jyoti Das, and M. Merchand, “Hunting for heavy  $Z'$  with IceCube neutrinos and gravitational waves,” [arXiv:2502.13217 \[hep-ph\]](#).
- [14] A. Boccia and F. Iocco, “A strike of luck: could the KM3-230213A event be caused by an evaporating



- primordial black hole?," [arXiv:2502.19245 \[astro-ph.HE\]](#).
- [15] D. Borah, N. Das, N. Okada, and P. Sarmah, "Possible origin of the KM3-230213A neutrino event from dark matter decay," [arXiv:2503.00097 \[hep-ph\]](#).
- [16] V. Brdar and D. S. Chattopadhyay, "Does the 220 PeV Event at KM3NeT Point to New Physics?," [arXiv:2502.21299 \[hep-ph\]](#).
- [17] K. Kohri, P. K. Paul, and N. Sahu, "Super heavy dark matter origin of the PeV neutrino event: KM3-230213A," [arXiv:2503.04464 \[hep-ph\]](#).
- [18] Y. Narita and W. Yin, "Explaining the KM3-230213A Detection without Gamma-Ray Emission: Cosmic-Ray Dark Radiation," [arXiv:2503.07776 \[hep-ph\]](#).
- [19] S. Jiang and F. P. Huang, "Pseudo-Goldstone Dark Matter from Primordial Black Holes: Gravitational Wave Signatures and Implications for KM3-230213A Event at KM3NeT," [arXiv:2503.14332 \[hep-ph\]](#).
- [20] G. F. S. Alves, M. Hostert, and M. Pospelov, "Neutron portal to ultra-high-energy neutrinos," [arXiv:2503.14419 \[hep-ph\]](#).
- [21] R. Wang and B.-Q. Ma, "Association of 220 PeV Neutrino KM3-230213A with Gamma-Ray Bursts," [arXiv:2503.14471 \[astro-ph.HE\]](#).
- [22] Y.-M. Yang, X.-J. Lv, X.-J. Bi, and P.-F. Yin, "Constraints on Lorentz invariance violation in neutrino sector from the ultra-high-energy event KM3-230213A," [arXiv:2502.18256 \[hep-ph\]](#).
- [23] K. Fang, F. Halzen, and D. Hooper, "Cascaded Gamma-ray Emission Associated with the KM3NeT Ultra-High-Energy Event KM3-230213A," *Astrophys. J. Lett.* **982** (2025) L16, [arXiv:2502.09545 \[astro-ph.HE\]](#).
- [24] P. Satunin, "Ultra-high-energy event KM3-230213A constraints on Lorentz Invariance Violation in neutrino sector," [arXiv:2502.09548 \[hep-ph\]](#).
- [25] T. A. Dzhatdoev, "The blazar PKS 0605-085 as the origin of the KM3-230213A ultra high energy neutrino event," [arXiv:2502.11434 \[astro-ph.HE\]](#).
- [26] A. Neronov, F. Oikonomou, and D. Semikoz, "KM3-230213A: An Ultra-High Energy Neutrino from a Year-Long Astrophysical Transient," [arXiv:2502.12986 \[astro-ph.HE\]](#).
- [27] G. Amelino-Camelia, G. D'Amico, G. Fabiano, D. Frattulillo, G. Gubitosi, A. Moia, and G. Rosati, "On testing in-vacuo dispersion with the most energetic neutrinos: KM3-230213A case study," [arXiv:2502.13093 \[astro-ph.HE\]](#).
- [28] M. Crnogorčević, C. Blanco, and T. Linden, "Looking for the  $\gamma$ -Ray Cascades of the KM3-230213A Neutrino Source," [arXiv:2503.16606 \[astro-ph.HE\]](#).
- [29] Y. Jho, S. C. Park, and C. S. Shin, "Superheavy Supersymmetric Dark Matter for the origin of KM3NeT Ultra-High Energy signal," [arXiv:2503.18737 \[hep-ph\]](#).
- [30] A. P. Klipfel and D. I. Kaiser, "Ultra-High-Energy Neutrinos from Primordial Black Holes," [arXiv:2503.19227 \[hep-ph\]](#).
- [31] K.-Y. Choi, E. Lkhagvadorj, and S. Mahapatra, "Cosmological Origin of the KM3-230213A event and associated Gravitational Waves," [arXiv:2503.22465 \[hep-ph\]](#).
- [32] A. Das, N. Okada, and D. Raut, "Enhanced pair production of heavy Majorana neutrinos at the LHC," *Phys. Rev.* **D97** no. 11, (2018) 115023, [arXiv:1710.03377 \[hep-ph\]](#).
- [33] P. Minkowski, " $\mu \rightarrow e\gamma$  at a Rate of One Out of  $10^9$  Muon Decays?," *Phys. Lett. B* **67** (1977) 421–428.
- [34] T. Yanagida, "Horizontal gauge symmetry and masses of neutrinos," *Conf. Proc.* **C7902131** (1979) 95–99.
- [35] M. Gell-Mann, P. Ramond, and R. Slansky, "Complex Spinors and Unified Theories," *Conf. Proc. C* **790927** (1979) 315–321, [arXiv:1306.4669 \[hep-th\]](#).
- [36] R. N. Mohapatra and G. Senjanovic, "Neutrino Mass and Spontaneous Parity Nonconservation," *Phys. Rev. Lett.* **44** (1980) 912. [,231(1979)].
- [37] J. Schechter and J. W. F. Valle, "Neutrino Masses in SU(2) x U(1) Theories," *Phys. Rev.* **D22** (1980) 2227.
- [38] O. Sawada and A. Sugamoto, eds., *Proceedings: Workshop on the Unified Theories and the Baryon Number in the Universe: Tsukuba, Japan, February 13-14, 1979*. Natl.Lab.High Energy Phys., Tsukuba, Japan, 1979.
- [39] R. N. Mohapatra and G. Senjanovic, "Neutrino Masses and Mixings in Gauge Models with Spontaneous Parity Violation," *Phys. Rev. D* **23** (1981) 165.
- [40] **Particle Data Group** Collaboration, S. Navas *et al.*, "Review of particle physics," *Phys. Rev. D* **110** no. 3, (2024) 030001.
- [41] L. J. Hall, K. Jedamzik, J. March-Russell, and S. M. West, "Freeze-In Production of FIMP Dark Matter," *JHEP* **03** (2010) 080, [arXiv:0911.1120 \[hep-ph\]](#).
- [42] H. B. Nielsen and P. Olesen, "Vortex Line Models for Dual Strings," *Nucl. Phys. B* **61** (1973) 45–61.
- [43] T. W. B. Kibble, "Topology of Cosmic Domains and Strings," *J. Phys. A* **9** (1976) 1387–1398.
- [44] A. Babul, T. Piran, and D. N. Spergel, "BOSONIC SUPERCONDUCTING COSMIC STRINGS. 1. CLASSICAL FIELD THEORY SOLUTIONS," *Phys. Lett. B* **202** (1988) 307–314.
- [45] A. Vilenkin and E. P. S. Shellard, *Cosmic Strings and Other Topological Defects*. Cambridge University Press, 7, 2000.
- [46] J. A. Dror, T. Hiramatsu, K. Kohri, H. Murayama, and G. White, "Testing the Seesaw Mechanism and Leptogenesis with Gravitational Waves," *Phys. Rev. Lett.* **124** no. 4, (2020) 041804, [arXiv:1908.03227 \[hep-ph\]](#).
- [47] A. Das, P. Konar, and S. Majhi, "Production of Heavy neutrino in next-to-leading order QCD at the LHC and beyond," *JHEP* **06** (2016) 019, [arXiv:1604.00608 \[hep-ph\]](#).
- [48] P. B. Pal and L. Wolfenstein, "Radiative Decays of Massive Neutrinos," *Phys. Rev. D* **25** (1982) 766.
- [49] R. E. Shrock, "Electromagnetic Properties and Decays of Dirac and Majorana Neutrinos in a General Class of Gauge Theories," *Nucl. Phys. B* **206** (1982) 359–379.
- [50] J. F. Navarro, C. S. Frenk, and S. D. M. White, "A Universal density profile from hierarchical clustering," *Astrophys. J.* **490** (1997) 493–508, [arXiv:astro-ph/9611107](#).
- [51] J. F. Navarro, E. Hayashi, C. Power, A. Jenkins, C. S. Frenk, S. D. M. White, V. Springel, J. Stadel, and T. R. Quinn, "The Inner structure of Lambda-CDM halos 3: Universality and asymptotic slopes," *Mon. Not. Roy. Astron. Soc.* **349** (2004) 1039, [arXiv:astro-ph/0311231](#).
- [52] J. Einasto and U. Haud, "Galactic models with massive

- corona. I - Method. II - Galaxy,” *aap* **223** no. 1-2, (Oct., 1989) 89–106.
- [53] A. W. Graham, D. Merritt, B. Moore, J. Diemand, and B. Terzic, “Empirical models for Dark Matter Halos. I. Nonparametric Construction of Density Profiles and Comparison with Parametric Models,” *Astron. J.* **132** (2006) 2685–2700, [arXiv:astro-ph/0509417](#).
- [54] A. Burkert, “The Structure of Dark Matter Halos in Dwarf Galaxies,” *apjl* **447** (July, 1995) L25–L28, [arXiv:astro-ph/9504041](#) [[astro-ph](#)].
- [55] F. W. Stecker, S. T. Scully, and M. A. Malkan, “An Empirical Determination of the Intergalactic Background Light from UV to FIR Wavelengths Using FIR Deep Galaxy Surveys and the Gamma-ray Opacity of the Universe,” *Astrophys. J.* **827** no. 1, (2016) 6, [arXiv:1605.01382](#) [[astro-ph.HE](#)]. [Erratum: *Astrophys. J.* 863, 112 (2018)].
- [56] C. W. Bauer, N. L. Rodd, and B. R. Webber, “Dark matter spectra from the electroweak to the Planck scale,” *JHEP* **06** (2021) 121, [arXiv:2007.15001](#) [[hep-ph](#)].
- [57] **LHAASO** Collaboration, Z. Cao *et al.*, “Measurement of Ultra-High-Energy Diffuse Gamma-Ray Emission of the Galactic Plane from 10 TeV to 1 PeV with LHAASO-KM2A,” *Phys. Rev. Lett.* **131** no. 15, (2023) 151001, [arXiv:2305.05372](#) [[astro-ph.HE](#)].
- [58] Y. A. Fomin, N. N. Kalmykov, I. S. Karpikov, G. V. Kulikov, M. Y. Kuznetsov, G. I. Rubtsov, V. P. Sulakov, and S. V. Troitsky, “Constraints on the flux of  $\sim (10^{16} - 10^{17.5})$  eV cosmic photons from the EAS-MSU muon data,” *Phys. Rev. D* **95** no. 12, (2017) 123011, [arXiv:1702.08024](#) [[astro-ph.HE](#)].
- [59] **Pierre Auger** Collaboration, A. Castellina, “Highlights from the Pierre Auger Observatory,” *PoS ICRC2019* (2021) 004, [arXiv:1909.10791](#) [[astro-ph.HE](#)].
- [60] **IceCube** Collaboration, R. Abbasi *et al.*, “The IceCube high-energy starting event sample: Description and flux characterization with 7.5 years of data,” *Phys. Rev. D* **104** (2021) 022002, [arXiv:2011.03545](#) [[astro-ph.HE](#)].
- [61] KM3NeT Collaboration, “KM3NeT Official Website,” 2025. <https://www.km3net.org/>. Accessed: 2025-04-01.
- [62] **IceCube** Collaboration, M. G. Aartsen *et al.*, “Differential limit on the extremely-high-energy cosmic neutrino flux in the presence of astrophysical background from nine years of IceCube data,” *Phys. Rev. D* **98** no. 6, (2018) 062003, [arXiv:1807.01820](#) [[astro-ph.HE](#)].
- [63] K. Kaneta, Z. Kang, and H.-S. Lee, “Right-handed neutrino dark matter under the  $B - L$  gauge interaction,” *JHEP* **02** (2017) 031, [arXiv:1606.09317](#) [[hep-ph](#)].
- [64] S. Ejima, O. Seto, and T. Shimomura, “Revisiting sterile neutrino dark matter in gauged  $U(1)_{B-L}$  model,” *Phys. Rev. D* **106** no. 10, (2022) 103513, [arXiv:2207.01775](#) [[hep-ph](#)].
- [65] O. Seto, T. Shimomura, and Y. Uchida, “Freeze-in sterile neutrino dark matter in feeble gauged  $B - L$  model,” [arXiv:2404.00654](#) [[hep-ph](#)].
- [66] **Particle Data Group** Collaboration, R. L. Workman *et al.*, “Review of Particle Physics,” *PTEP* **2022** (2022) 083C01.
- [67] **Planck** Collaboration, N. Aghanim *et al.*, “Planck 2018 results. VI. Cosmological parameters,” *Astron. Astrophys.* **641** (2020) A6, [arXiv:1807.06209](#) [[astro-ph.CO](#)]. [Erratum: *Astron. Astrophys.* 652, C4 (2021)].
- [68] C. Ringeval, M. Sakellariadou, and F. Bouchet, “Cosmological evolution of cosmic string loops,” *JCAP* **02** (2007) 023, [arXiv:astro-ph/0511646](#).
- [69] J. J. Blanco-Pillado, K. D. Olum, and B. Shlaer, “Large parallel cosmic string simulations: New results on loop production,” *Phys. Rev. D* **83** (2011) 083514, [arXiv:1101.5173](#) [[astro-ph.CO](#)].
- [70] A. Vilenkin, “Gravitational radiation from cosmic strings,” *Phys. Lett. B* **107** (1981) 47–50.
- [71] T. Vachaspati and A. Vilenkin, “Gravitational Radiation from Cosmic Strings,” *Phys. Rev. D* **31** (1985) 3052.
- [72] J. J. Blanco-Pillado, K. D. Olum, and B. Shlaer, “The number of cosmic string loops,” *Phys. Rev. D* **89** no. 2, (2014) 023512, [arXiv:1309.6637](#) [[astro-ph.CO](#)].
- [73] J. J. Blanco-Pillado and K. D. Olum, “Stochastic gravitational wave background from smoothed cosmic string loops,” *Phys. Rev. D* **96** no. 10, (2017) 104046, [arXiv:1709.02693](#) [[astro-ph.CO](#)].
- [74] C. J. A. P. Martins and E. P. S. Shellard, “Quantitative string evolution,” *Phys. Rev. D* **54** (1996) 2535–2556, [arXiv:hep-ph/9602271](#).
- [75] C. J. A. P. Martins and E. P. S. Shellard, “Extending the velocity dependent one scale string evolution model,” *Phys. Rev. D* **65** (2002) 043514, [arXiv:hep-ph/0003298](#).
- [76] P. Auclair *et al.*, “Probing the gravitational wave background from cosmic strings with LISA,” *JCAP* **04** (2020) 034, [arXiv:1909.00819](#) [[astro-ph.CO](#)].
- [77] T. Damour and A. Vilenkin, “Gravitational wave bursts from cusps and kinks on cosmic strings,” *Phys. Rev. D* **64** (2001) 064008, [arXiv:gr-qc/0104026](#).
- [78] Y. Gouttenoire, G. Servant, and P. Simakachorn, “Beyond the Standard Models with Cosmic Strings,” *JCAP* **07** (2020) 032, [arXiv:1912.02569](#) [[hep-ph](#)].
- [79] A. Vilenkin, “Cosmic string dynamics with friction,” *Phys. Rev. D* **43** (1991) 1060–1062.
- [80] J. Crowder and N. J. Cornish, “Beyond LISA: Exploring future gravitational wave missions,” *Phys. Rev. D* **72** (2005) 083005, [arXiv:gr-qc/0506015](#).
- [81] V. Corbin and N. J. Cornish, “Detecting the cosmic gravitational wave background with the big bang observer,” *Class. Quant. Grav.* **23** (2006) 2435–2446, [arXiv:gr-qc/0512039](#).
- [82] N. Seto, S. Kawamura, and T. Nakamura, “Possibility of direct measurement of the acceleration of the universe using 0.1-Hz band laser interferometer gravitational wave antenna in space,” *Phys. Rev. Lett.* **87** (2001) 221103, [arXiv:astro-ph/0108011](#).
- [83] H. Kudoh, A. Taruya, T. Hiramatsu, and Y. Himemoto, “Detecting a gravitational-wave background with next-generation space interferometers,” *Phys. Rev. D* **73** (2006) 064006, [arXiv:gr-qc/0511145](#).
- [84] **LISA** Collaboration, P. Amaro-Seoane *et al.*, “Laser Interferometer Space Antenna,” [arXiv:1702.00786](#) [[astro-ph.IM](#)].
- [85] D. Reitze *et al.*, “Cosmic Explorer: The U.S. Contribution to Gravitational-Wave Astronomy beyond LIGO,” *Bull. Am. Astron. Soc.* **51** no. 7, (2019) 035, [arXiv:1907.04833](#) [[astro-ph.IM](#)].
- [86] S. Hild *et al.*, “Sensitivity Studies for Third-Generation Gravitational Wave Observatories,” *Class. Quant. Grav.*

- [28](#) (2011) 094013, [arXiv:1012.0908 \[gr-qc\]](#).
- [87] M. Punturo *et al.*, “The Einstein Telescope: A third-generation gravitational wave observatory,” *Class. Quant. Grav.* **27** (2010) 194002.
- [88] B. Sathyaprakash *et al.*, “Scientific Objectives of Einstein Telescope,” *Class. Quant. Grav.* **29** (2012) 124013, [arXiv:1206.0331 \[gr-qc\]](#). [Erratum: *Class.Quant.Grav.* 30, 079501 (2013)].
- [89] M. Maggiore *et al.*, “Science Case for the Einstein Telescope,” *JCAP* **03** (2020) 050, [arXiv:1912.02622 \[astro-ph.CO\]](#).
- [90] T. Charnock, A. Avgoustidis, E. J. Copeland, and A. Moss, “CMB constraints on cosmic strings and superstrings,” *Phys. Rev. D* **93** no. 12, (2016) 123503, [arXiv:1603.01275 \[astro-ph.CO\]](#).
- [91] **NANOGrav** Collaboration, A. Afzal *et al.*, “The NANOGrav 15 yr Data Set: Search for Signals from New Physics,” *Astrophys. J. Lett.* **951** no. 1, (2023) L11, [arXiv:2306.16219 \[astro-ph.HE\]](#). [Erratum: *Astrophys.J.Lett.* 971, L27 (2024), Erratum: *Astrophys.J.* 971, L27 (2024)].
- [92] A. Esmaili, S. K. Kang, and P. D. Serpico, “IceCube events and decaying dark matter: hints and constraints,” *JCAP* **12** (2014) 054, [arXiv:1410.5979 \[hep-ph\]](#).
- [93] T. Higaki, R. Kitano, and R. Sato, “Neutrino Universe,” *JHEP* **07** (2014) 044, [arXiv:1405.0013 \[hep-ph\]](#).

# Supplemental Material

Basabendu Barman, Arindam Das, Prantik Sarmah

## I. INTERACTIONS AND DECAY WIDTHS

Under the general  $U(1)_X$  scenario left- and right-handed fermions interact differently with the  $Z'$  and the interaction Lagrangian manifest chiral scenario involving their general  $U(1)_X$  charges. We write the interactions Lagrangian as

$$\mathcal{L} = -g_X (\bar{f} \gamma^\mu q_{f_L} P_L f + \bar{f} \gamma^\mu q_{f_R} P_R f) Z'_\mu, \quad (29)$$

where  $P_{L(R)} = (1 \mp \gamma_5)/2$  is the left- (right-)handed projections and  $q_{f_{L(R)}}$  is the corresponding general  $U(1)_X$  charge of the left- (right-)handed fermion ( $f_{L(R)}$ ). The partial decay widths of  $Z'$  into a pair of charged fermions can be written as

$$\Gamma(Z' \rightarrow \bar{f}f) = N_C \frac{M_{Z'} g_X^2}{24\pi} \left[ (q_{f_L}^2 + q_{f_R}^2) \left( 1 - \frac{m_f^2}{M_{Z'}^2} \right) + 6q_{f_L} q_{f_R} \frac{m_f^2}{M_{Z'}^2} \right] \left( 1 - 4 \frac{m_f^2}{M_{Z'}^2} \right)^{\frac{1}{2}}, \quad (30)$$

where  $m_f$  is the mass of the SM fermions and  $N_C = 1(3)$  is the color factor for the SM leptons (quarks). For heavy  $Z'$  ion the TeV scale and above, the effect of the SM masses can be neglected. The partial decay width of  $Z'$  into a pair of light neutrinos ( $\nu_L$ ) can be written as

$$\Gamma(Z' \rightarrow \nu\nu) = \frac{M_{Z'} g_X^2}{24\pi} q_{\ell_L}^2, \quad (31)$$

neglecting the tiny light neutrino mass and  $q_{\ell_L}$  is the  $U(1)_X$  charge of the SM lepton doublets. The  $Z'$  gauge boson can decay into a pair of heavy Majorana neutrinos if  $M_{Z'} > M_{N_\beta}/2$ . The kinematically allowed partial decay width of  $Z'$  into one generation of heavy neutrino pair can be given by

$$\Gamma(Z' \rightarrow N_\beta N_\beta) = \frac{M_{Z'} g_X^2}{24\pi} q_{N_R}^2 \left( 1 - 4 \frac{M_{N_\beta}^2}{M_{Z'}^2} \right)^{\frac{3}{2}}, \quad (32)$$

where  $q_{N_R}$  is the general  $U(1)_X$  charge of the heavy neutrinos. If we consider the scenario where  $M_{N_\beta} > M_{Z'}/2$ , then  $Z' \rightarrow N_\beta N_\beta$  mode will be absent. In addition we write the dominant decay rates of the BSM scalar  $\phi$  into a pair of  $Z'$  from the kinetic term and into a pair of RHNs from the Yukawa interaction as

$$\Gamma_{\phi \rightarrow Z' Z'} = \frac{g_X^2}{8\pi r^4} \frac{M_{Z'}^2}{m_\phi} \sqrt{1 - 4r^2} (12r^4 - 4r^2 + 1) \quad (33)$$

$$\Gamma_{\phi \rightarrow N_\beta N_\beta} = \frac{g_X^2}{2\pi} \left( \frac{M_{N_\beta}}{M_{Z'}} \right)^2 m_\phi \left( 1 - \frac{4M_{N_\beta}^2}{m_\phi^2} \right)^{3/2} \quad (34)$$

where  $r = M_{Z'}/m_\phi$ .

## II. NEUTRINO MASS

In order to generate the neutrino mass from the seesaw mechanism, the neutrino mass matrix can be written as

$$\mathcal{M}_\nu = \begin{pmatrix} 0 & M_D \\ M_D^T & M_N \end{pmatrix}. \quad (35)$$

Assuming the hierarchy of  $|M_{D_{ij}}/M_{N_\beta}| \ll 1$ , we diagonalize the neutrino mass matrix to obtain the non-zero neutrino mass eigenvalue of light Majorana neutrino as

$$m_\nu \simeq -M_D M_N^{-1} M_D^T. \quad (36)$$

which is the well known seesaw formula. Due to the light-heavy neutrino mixing from the seesaw mechanism, a flavor eigenstate of light neutrino ( $\nu_\alpha$ ) can be written as a linear combination of the mass eigenstates of light ( $\nu_i$ ) and heavy ( $N_i$ ) neutrino

$$\nu_\alpha \simeq \mathcal{U}_{\alpha i} \nu_i + V_{\alpha i} N_i, \quad (37)$$

where  $\mathcal{U}$ , the PMNS matrix, is taken at the leading order after ignoring the non-unitarity effects for simplicity. Now we diagonalize the light neutrino mass matrix as

$$\mathcal{U}^T m_\nu \mathcal{U} = \text{diag}(m_1, m_2, m_3). \quad (38)$$

where PMNS matrix can be given by

$$\mathcal{U} = \begin{pmatrix} C_{12}C_{13} & S_{12}C_{13} & S_{13}e^{i\delta} \\ -S_{12}C_{23} - C_{12}S_{23}S_{13}e^{i\delta} & C_{12}C_{23} - S_{12}S_{23}S_{13}e^{i\delta} & S_{23}C_{13} \\ S_{12}C_{23} - C_{12}C_{23}S_{13}e^{i\delta} & -C_{12}S_{23} - S_{12}C_{23}S_{13}e^{i\delta} & C_{23}C_{13} \end{pmatrix} \begin{pmatrix} 1 & 0 & 0 \\ 0 & e^{i\rho_1} & 0 \\ 0 & 0 & e^{i\rho_2} \end{pmatrix} \quad (39)$$

with  $C_{ij} = \cos\theta_{ij}$ ,  $S_{ij} = \sin\theta_{ij}$ ,  $\delta(\rho_{1,2})$  is the Dirac(Majorana)  $CP$  phase. In this analysis we adopt neutrino oscillation data as  $\sin^2 2\theta_{13} = 0.092$ ,  $\sin^2 2\theta_{12} = 0.87$ ,  $\sin^2 2\theta_{23} = 1.0$ ,  $\Delta m_{12}^2 = m_2^2 - m_1^2 = 7.6 \times 10^{-5} \text{ eV}^2$ , and  $|\Delta m_{23}^2| = |m_3^2 - m_2^2| = 2.4 \times 10^{-3} \text{ eV}^2$  from [40] for the NH and IH cases. Now we write the mixing between the light and heavy neutrino mass eigenstates in the seesaw scenario following general parametrization as

$$V^{\text{NH/IH}} = \mathcal{U}^* \sqrt{D^{\text{NH/IH}}} \mathcal{O} \sqrt{M_N^{-1}}, \quad (40)$$

where  $\mathcal{O}$  is a general orthogonal matrix:

$$\mathcal{O} = \begin{pmatrix} 1 & 0 & 0 \\ 0 & \cos x & \sin x \\ 0 & -\sin x & \cos x \end{pmatrix} \begin{pmatrix} \cos y & 0 & \sin y \\ 0 & 1 & 0 \\ -\sin y & 0 & \cos y \end{pmatrix} \begin{pmatrix} \cos z & \sin z & 0 \\ -\sin z & \cos z & 0 \\ 0 & 0 & 1 \end{pmatrix} \quad (41)$$

with the angles,  $x, y, z$  being complex numbers, and  $D_{\text{NH/IH}}$  is the light neutrino mass eigenvalue matrix

$$D^{\text{NH}} = \text{diag}(m_{\text{lightest}}, m_2^{\text{NH}}, m_3^{\text{NH}}), \quad D^{\text{IH}} = \text{diag}(m_1^{\text{IH}}, m_2^{\text{IH}}, m_{\text{lightest}}) \quad (42)$$

with  $m_2^{\text{NH}} = \sqrt{\Delta m_{12}^2 + m_{\text{lightest}}^2}$ ,  $m_3^{\text{NH}} = \sqrt{\Delta m_{23}^2 + (m_2^{\text{NH}})^2}$ ,  $m_2^{\text{IH}} = \sqrt{\Delta m_{23}^2 + m_{\text{lightest}}^2}$  and  $m_1^{\text{IH}} = \sqrt{(m_2^{\text{IH}})^2 - \Delta m_{12}^2}$ . In both cases, the RHN mass matrix is defined as  $M_N = \text{diag}(M_{N_1}, M_{N_2}, M_{N_3})$ . Hence, the mixing matrix  $V$  in Eq. (7) becomes a function of  $\rho_{1,2}$ ,  $m_{\text{lightest}}$ ,  $M_{N_\beta}$  ( $\beta = 1, 2, 3$ ), the three complex angles and neutrino oscillation data. For a simple parametrization one can consider that  $x, y, z = 0$  making  $\mathcal{O}$  an identity matrix. Now the modified charged-current (CC) interaction in the lepton sector can be written as

$$\mathcal{L}_{\text{CC}} = -\frac{g}{\sqrt{2}} W_\mu \bar{\ell} \gamma^\mu P_L [\mathcal{U}_{\alpha i} \nu_i + V_{\alpha i} N_i] + \text{H.c.}, \quad (43)$$

where  $g$  is the  $SU(2)_L$  gauge coupling and the modified neutral-current (NC) interaction in the lepton sector will be

$$\mathcal{L}_{\text{NC}} = -\frac{g}{2 \cos \theta_w} Z_\mu [(\mathcal{U}^\dagger \mathcal{U})_{ij} \bar{\nu}_i \gamma^\mu P_L \nu_j + (\mathcal{U}^\dagger V)_{ki} \bar{\nu}_k \gamma^\mu P_L N_i + (V^\dagger V)_{mi} \bar{N}_m \gamma^\mu P_L N_i] + \text{H.c.}, \quad (44)$$

where  $\theta_w$  is the weak mixing angle.

### III. CROSS-SECTION

For charged lepton initial states,

$$\sigma(s)_{\ell^+ \ell^- \rightarrow \text{DMDM}} \simeq \frac{g_X^4}{96\pi [(s - M_{Z'}^2)^2 + \Gamma_{Z'}^2, M_{Z'}^2]} \sqrt{1 - \frac{4M_{N_1}^2}{s}} x_\Phi^2 \frac{(s - 4M_{N_1}^2)(5x_H^2 + 12x_H x_\Phi + 8x_\Phi^2)}{2}. \quad (45)$$



For light neutrino initial states

$$\sigma(s)_{\nu\nu\rightarrow\text{DMDM}} \simeq \frac{g_X^4}{48\pi [(s - M_{Z'}^2)^2 + \Gamma_{Z'}^2 M_{Z'}^2]} \sqrt{1 - \frac{4 M_{N_1}^2}{s}} x_\Phi^2 \frac{(s - 4 M_{N_1}^2) (x_H + 2 x_\Phi)^2}{4} \quad (46)$$

For up-quark initial states,

$$\sigma(s)_{uu\rightarrow\text{DMDM}} \simeq x_\Phi^2 \frac{(s - 4 M_{N_1}^2) (17 x_H^2 + 20 x_H x_\Phi + 8 x_\Phi^2)}{2}. \quad (47)$$

For down-quark initial states,

$$\sigma(s)_{dd\rightarrow\text{DMDM}} \simeq x_\Phi^2 \frac{(s - 4 M_{N_1}^2) (5 x_H^2 - 4 x_H x_\Phi + 8 x_\Phi^2)}{2}. \quad (48)$$

#### IV. BOLTZMANN EQUATIONS

The coupled BEQs for freeze-in production of the DM read,

$$\begin{aligned} \frac{dy_\phi}{dz} &= -\frac{z}{\mathcal{H}} \langle \Gamma_\phi \rangle y_{\text{eq}}^\phi + \frac{s}{\mathcal{H}} \frac{1}{z^2} \langle \sigma v \rangle_{\text{SM SM} \rightarrow \phi \phi} (y_{\text{eq}}^\phi)^2, \\ \frac{dy_{Z'}}{dz} &= -\frac{z}{\mathcal{H}} \langle \Gamma_{Z'} \rangle y_{Z'} + \frac{z}{\mathcal{H}} \langle \Gamma_{\phi \rightarrow Z' Z'} \rangle (y_{\text{eq}}^\phi - y_{Z'}), \\ \frac{dy_{N_1}}{dz} &= \frac{z}{\mathcal{H}} \langle \Gamma_{Z' \rightarrow N_1 N_1} \rangle y_{Z'} + \frac{z}{\mathcal{H}} \langle \Gamma_{\phi \rightarrow N_1 N_1} \rangle y_{\text{eq}}^\phi + \frac{s}{\mathcal{H}} \frac{1}{z^2} \langle \sigma v \rangle_{\text{SM SM} \rightarrow N_1 N_1} y_{\text{eq}}^2, \end{aligned} \quad (49)$$

where  $y_i \equiv n_i/s$  is the yield of a certain species  $i$ , with

$$y_j^{\text{eq}} = \frac{45}{4\pi^4} \frac{g_j}{g_{\star s}} z^2 K_2[z], \quad (50)$$

is the equilibrium yield, with  $g_j$  being the degrees of freedom for the corresponding  $j$  particle and  $z = M_1/T$  is a dimensionless variable. Here,  $\mathcal{H} = (\pi/3) \sqrt{g_\star/10} (T^2/M_P)$  is the Hubble parameter for a standard radiation dominated (RD) Universe and  $s = (2\pi^2/45) g_{\star s}(T) T^3$  is the entropy density. The number of relativistic degrees of freedom in the bath corresponding to energy density and entropy density are tracked by  $g_\star(T)$  and  $g_{\star s}(T)$ , respectively. At temperatures well above the QCD phase transition we have  $g_\star(T) \simeq g_{\star s}(T) \approx 106$ . The thermally averaged decay rate is given by

$$\langle \Gamma_{\phi \rightarrow jj} \rangle = \frac{K_1(z)}{K_2(z)} \times \Gamma_{\phi \rightarrow jj}, \quad (51)$$

with  $z = M_1/T$ , and  $j$  represents the final state particle.